

This item was submitted to Loughborough's Institutional Repository (<https://dspace.lboro.ac.uk/>) by the author and is made available under the following Creative Commons Licence conditions.



CC creative commons
COMMONS DEED

Attribution-NonCommercial-NoDerivs 2.5

You are free:

- to copy, distribute, display, and perform the work

Under the following conditions:

 **Attribution.** You must attribute the work in the manner specified by the author or licensor.

 **Noncommercial.** You may not use this work for commercial purposes.

 **No Derivative Works.** You may not alter, transform, or build upon this work.

- For any reuse or distribution, you must make clear to others the license terms of this work.
- Any of these conditions can be waived if you get permission from the copyright holder.

Your fair use and other rights are in no way affected by the above.

This is a human-readable summary of the [Legal Code \(the full license\)](#).

[Disclaimer](#) 

For the full text of this licence, please go to:
<http://creativecommons.org/licenses/by-nc-nd/2.5/>

Influence of Laser beam Brightness during Surface Treatment of a ZrO₂ Engineering Ceramic

P. P. Shukla^{*}, J. Lawrence[✉] and A. Paul[✉]

Jonathan Lawrence[✉], Lincoln School of Engineering, University of Lincoln, Brayford Pool, Lincoln,
LN6 7TS, United Kingdom

Anish Paul[✉], Loughborough University, Department of Materials, Leicestershire, LE11 3TU, United
Kingdom.

Correspondence Address:

Pratik P. Shukla^{*}, Loughborough University, Wolfson School of Mechanical and Manufacturing
Engineering, Leicestershire, LE11 3TU, United Kingdom, Email: P.Shukla@lboro.ac.uk, Direct Line: +44
(0) 1509227592

Abstract

A comparative study between fibre and Nd:YAG (neodymium, yttrium, aluminium, garnet) laser surface treatment on a cold isostatic pressed (CIP) ZrO₂ engineering ceramic was conducted to investigate the individual differences of laser brightness (radiance) produced by the two laser sources. The effects of brightness exhibited by the two lasers were investigated in respect to the change in the hardness, dimensional size of the laser radiated zones and the microstructure of the ZrO₂ engineering ceramic. The results showed that the hardness of the ZrO₂ engineering ceramic was reduced by 36% for the Nd:YAG laser in comparison to the as-received surface. However, only 4% reduction in the surface hardness was found from employing the fibre laser surface treatment which was not significant as much as the results of the Nd:YAG laser radiation. The change in hardness occurred due to softening of the laser radiated surface of the ZrO₂ with a changed composition which was softer than the laser unaffected surface. The dimensional size of the fibre laser radiated track was also found to produce broader surface profiles in comparison to that of the Nd:YAG laser. The fibre laser radiated surface track was 32% larger in width and 51.5% longer in depth of penetration in comparison to that of the Nd:YAG laser. Change in microstructure of the ZrO₂ engineering ceramic radiated by both lasers was found as opposed to the ground and polished untreated surface with the fibre laser affecting the grain morphology to a greater extent in comparison to that of the Nd:YAG laser radiation. The physical and micro-structural effects from applying the two laser types to the ZrO₂ engineering ceramic differed as deep penetration and broader laser radiated track as well as larger grains were produced by the fibre laser, despite using identical laser processing parameters such as spot size, power density, traverse speed, gas flow rate, wavelength and the Gaussian beam profile. This occurred due to the high brightness exhibited by the fibre laser radiation which generated larger power per unit area which in turn induced into the ZrO₂ engineering ceramic and resulted to producing high processing temperature, larger fibre laser-ceramic-interaction zone and melt-pool at the laser-ZrO₂ interface in comparison to that of the Nd:YAG laser which intrinsically resulted to a change in physical attributes of the ceramic.

Keywords: Nd:YAG laser; Fibre laser; Brightness; ZrO₂ engineering ceramic.

1. Introduction

Brightness is a very important characteristic of a light source. It is defined as the amount of light delivered from a surface per unit of area [1, 2]. The term brightness is mainly used when the visual quality of a light source in relation to contrast and glare is being expressed. However, brightness in turn does not only relate to a light source such as a lamp or a candle as light can be found through reflection and transmission also. For instance, a bright surface will have high reflections and a dull surface will have low reflection [1, 2]. The use of the term brightness in some way or another is a comparison of two light sources which are judged by the human eye as it creates variation in the intensities on the surface of the retina [3].

Brightness in general terms is defined as candles per square meter of light being emitted on a surface and is classified as “luminance” or “radiance” depending its application [2, 4]. When the brightness is mentioned as a photometric quantity the term luminance is usually used. However, the term radiance is mentioned when describing radiometric quantity [4]. Luminance can be expressed as the direction of light emission. This means that the brightness of an object is dependent on the direction or the angle which one can look from [1, 2]. Luminance is also the intensity of light that is emitted from the surface whereas the intensity of light that is directed on a surface is classified as illuminance which is the opposite of luminance. In some instance, radiometric term radiance of a light source is used in literatures for the sake of simplicity particularly when expressing laser beam brightness which is the power per unit area per solid angle of divergence [1, 2].

Laser beams in comparison to other light sources comprise of high brightness energy since a laser light exhibits very high power levels in a narrow beam or a spot size [3]. Hence, the spot size which the laser beam can be focused to is very important [5]. Brightness of lasers is an unchangeable property which means that the brightness is not affected by focusing or defocusing a light beam. This is made clear by a primary law of optics which states that the brightness of a light source is an unchangeable quantity [2, 6]. The brightness of a Gaussian beam does not change as it propagates because the brightness is inversely proportion to the solid angle. The solid angle produced by a laser beam is proportional to the square of the divergence angle θ ; the smaller the divergence the higher the brightness. High brightness beams, however, has the most idealised beam profile and tend to have a high beam quality factor.

Laser power density and laser brightness has close relationship due to their parameters being somewhat common: the laser power is input power per spot size which is multiplied by the Gaussian beam configuration value whereas the brightness is the input power per unit area per solid angle (beam divergence) [7 - 10]. Brightness is important in laser processing applications since the intensity obtained within a focusing area within a lens is proportional to the brightness of the beam. High brightness laser processing allows fine spot size of the beam and allows longer focusing distance so that flexibility is further achieved with material processing as more distance is covered during the laser processing. This is particularly offered by the fibre laser and are both used for the investigation herein as further presented in this study.

High brightness laser sources such as a fibre laser or a high powered diode laser (HPDL) produce high temperature during material interaction [8, 11]. High brightness laser source in particular –a fibre laser also offer a longer depth of field (long focal length), small spot sizes and beam quality as well as stability during laser execution. The brightness of a laser is more effective in comparison to the laser power intensity. This is because by achieving a high brightness would generate high processing temperatures [11]. This is particularly important for ceramic processing in order to achieve surface melting, to cover the surface cracks and to achieve localized modification and phase transformations within the ceramic. The use of high brightness laser for material processing is also advantageous due to its potential of achieving low cost per wattage output [4].

Measuring the brightness of a light source is a difficult practice and requires a complex set-up and procedures to follow. This is specially so for measuring the brightness of an industrial laser due to the complexity of the machines and the experimental set-up required. The correct measuring technique for brightness of a laser beam is strategically documented in the British standards [12 - 14]. Forbes *et al.* [15] modelled the brightness from a cross porro-prism resonators and showed that the brightness is significantly influenced by the angle between the two prism edges. At higher prism angles the brightness was increased as fewer petals of the beam footprint were to be seen, with decreasing angles and increasing the number of petals of the beam footprint showed decreasing the prism angles and inherently a reduction in the brightness.

The use of high brightness emitting lasers have made a way forward within the laser aided material processing industry in the recent years, which has been reported on by several

workers. Wallace [16] described the use of high brightness beam diode lasers which produces high efficiencies and lower operating costs. Wnzel *et al.* [17] modelled features of high brightness semiconductor lasers and showed that high reliability and efficiency can be obtained from applying high brightness laser beam despite having low beam quality. Brown and Frye [18] also showed the use of high brightness cutting and drilling of aerospace materials by using a Nd:YAG (neodymium, yttrium, aluminium garnet) laser. The results showed improved cutting and also achieved shallow angle holes. Li *et al.* [19] investigated the reliability and efficiency of high brightness lasers of 940 nm wavelength and demonstrated the maximum power conversion efficiency of 60% at an output power of 72 W with very good beam quality. Treusch *et al.* [20] studied the use of high-brightness semiconductor lasers for material processing and revealed that collimation lenses can be used to increase the brightness of the laser by a factor of two as well as the wavelength and polarization coupling also contributing to the increased brightness. Leibreich and Treusch [21] followed a similar investigation on improving the brightness of a semiconductor diode laser by using stacking laser bars (beams) comprising of different wavelength to increase the output power as well as the brightness. Their results briefly described that the brightness can be enhanced by two without any changes to the beam quality factor (M^2) which in turn would improve and open a new avenue for the laser materials processing sector. Other investigation by Hanna [22, 23] showed that an increase in brightness can be obtained by altering the transverse mode. Variation in the transverse mode leads to a change in the beam divergence and alters the brightness of the laser source [22].

Val *et al.* [24] investigated the effects of laser cladding of flat plates of AISI 304 stainless steel and Co-based super-alloy powder as a coating material by applying a Nd:YAG laser and a Yb: YAG fibre laser. The results from the fibre laser in comparison to that of the Nd:YAG showed more versatility with regard to the parameter window as well as enlarged clad track, and deeper penetration. However, similar hardness was obtained from applying both laser types. Val *et al.* further concluded that this effect had occurred due to the better beam quality and also due to the high brightness on offer by the fibre laser which is ideal for producing narrower clad tracks and a Nd:YAG laser – ideal for producing wider clad tracks. The work of Val *et al.* closely relates to the work in this study as the effects of brightness between an Nd:YAG laser and a fibre laser are investigated but by using engineering ceramics (in particular ZrO_2).

Although, several investigations have been published in the field of improving the laser brightness, there is still limited work that has been published with the use of a fibre laser to process materials. This is particularly so for engineering ceramics as up till date, no work has been conducted hitherto with employing the fibre laser surface treatment on engineering ceramics which considers the laser brightness as an influential feature of laser-ceramic and other material processing in general and the physical effect of its surface interaction with such materials. Also, brightness is an important parameter of laser material processing rather than the input power. It is the brightness that is the driving force rather than the power intensity and is very much discarded when it come to laser material processing. Hence, the work in this investigation attempts to introduce the likely effects which can occur by the different brightness of laser sources as they yet have the same input parameters. Physical differences in the effects of the fibre laser and the Nd:YAG laser brightness up on surface treatment of the ZrO₂ engineering ceramics in particular is discussed after the laser-ceramic surface interaction has taken place.

2. Fundamentals of Laser Brightness

Theoretical brightness is calculated by means of simplified equations described in numerous literatures [2-7]:

$$\mathbf{Br} = \frac{P_{out}}{A\Omega} \quad (1)$$

Where P_{out} is the power over the surface area and Ω is the solid angle of divergence of the beam. Brightness is inversely equal to the solid angle of divergence. The solid angle of divergence created by a laser beam is equal to the square of the divergence angle θ as shown in Figure 1. The solid angle of a Gaussian beam equates to:

$$\Omega = \pi \theta^2 = \lambda^2 / \pi w_0^2 \quad (2)$$

and is inversely proportional to (πw_0^2) . Where λ is the wavelength of the particular laser beam and w_0 is the beam radius at the beam waist or divergence. The solid angle of divergence is usually small for laser beams in comparison to other light sources due to their high directionality and this in turn generates high brightness beams.

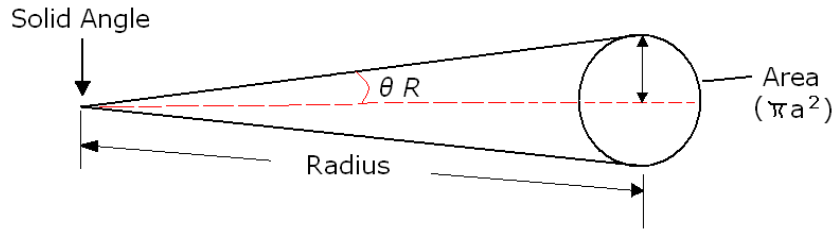


Figure 1 Schematic diagram illustrating the solid angle of divergence of a laser beam.

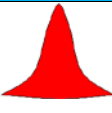

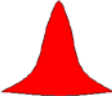

For a circular Gaussian laser beam; the beam propagation ratio is illustrated in Equation 3. Where M_y^2 and M_x^2 are the beam propagation ratio's in the X and the Y direction. Furthermore, brightness can be derived in Equation 4 which comprises of feature in Equation 1 and 2 3:

$$M^4 = M_y^2 \cdot M_x^2 \quad (3)$$

$$Br = \frac{P_{out}}{M^4 \times \lambda^2} \quad (4)$$

The solid angle presented in Figure 1 is a unique dimension for all laser beams with different beam profile and Gaussian configuration. This solid angle is the divergence of the beam after being focused by the optics (focusing lens). The angle of beam divergence the calculated brightness values of the fibre laser and the Nd:YAG laser are presented in Table 1, along with other beam characteristics and properties as a comparison.

Table 1 Properties of the fibre and Nd:YAG lasers used for this investigation.

Laser type	Beam divergence (m/rad)	Brightness ($W/cm^2 / sr^{-1}$)	Beam quality factor (M^2)	Gaussian beam shape		Gaussian mode
				Cross-sectional view	Plan view	
Nd:YAG laser	5.5	609.50	6.8			TEM ₀₀
Fibre laser	0.2	1855.37	1.2			TEM ₀₀

3. Experimentation and Analysis

3.1 Experimental Materials

The material used for the experimentation was cold isostatic pressed (CIP) ZrO₂ with 95 wt% ZrO₂ and 5 wt% yttria (Tensky International Company, Ltd). Each test piece was obtained in a bulk of 10 x 10 x 50 mm³ (see Figure 2) with a surface roughness of 1.58 μm (as-received from the manufacturer). This was to reduce the laser beam reflection as the well polished shinier surfaces of the ceramic would reduce beam absorption. The experiments were conducted in ambient condition at a known temperature (25°C). All surfaces of the ZrO₂ to be treated were marked with black ink prior to the laser treatment to enhance the absorption and allow the laser beam to further penetrate into the surface.

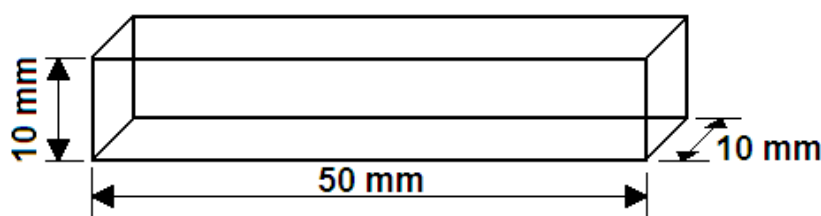


Figure 2 Schematic diagram of the experimental work-piece of the Si₃N₄ engineering ceramic.

3.2 Nd:YAG laser surface treatment

A 65 W Nd:YAG laser (HK, SL902; Hahn & Kolb Ltd.) emitting a continuous wave (CW) mode beam at a wavelength of 1.064 μm was used in this work (see Figure 3). The focal position was kept to 210 mm above the work-piece to obtain a 2.2 mm spot size. The processing gases used was N₂ at a flow rate of 25 l/min. Programming of the laser was conducted using a Hahn & Kolb, U3 CAD software which integrated with the laser system as a 50 mm line was programmed using numerical control (NC) programming as a potential beam path. To obtain an operating window, trials were conducted at the fixed spot size of 2.2 mm and 65 W by varying the speed between 4 and 100 mm/sec. From these trials it was found that 10 mm/sec at 65 W were the ideal laser parameter to use in terms of achieving a sufficient footprint on the material to conduct further analysis.

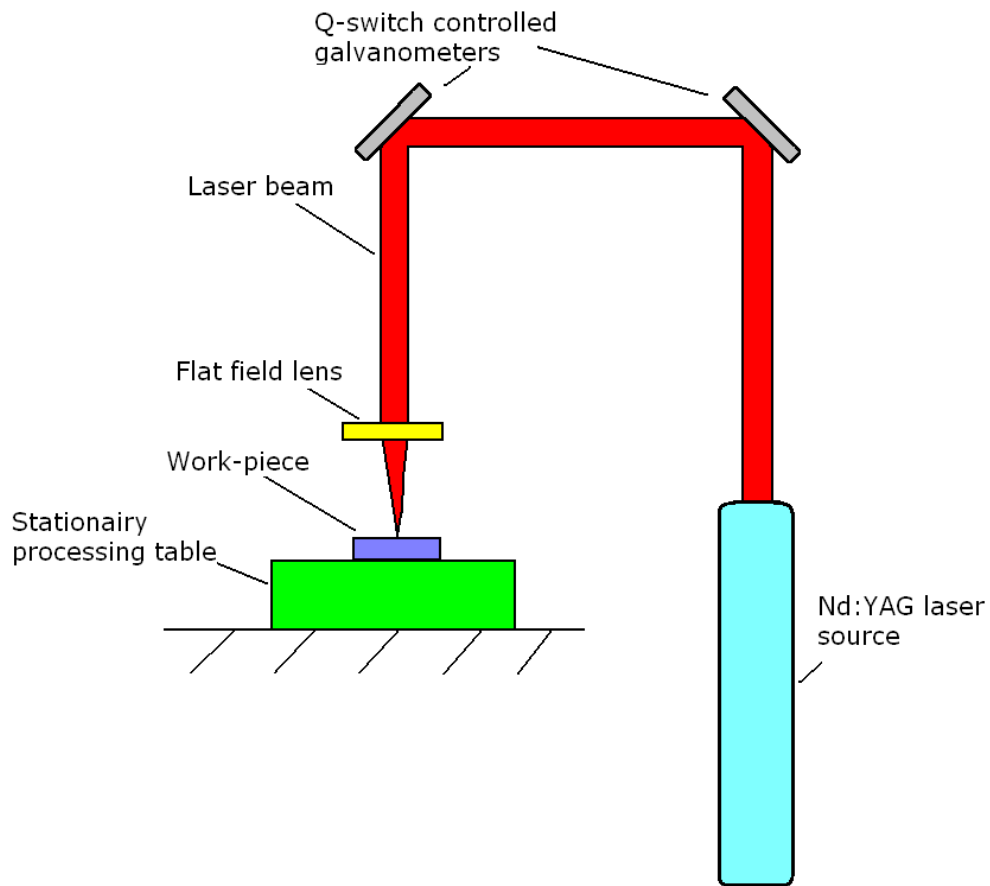


Figure 3 Schematic diagram showing the experimental set-up of the fibre laser surface treatment of the ZrO₂ engineering ceramic.

3.3 Fibre laser surface treatment

A 200 W fibre laser (SPI-200c-002; SPI, Ltd.) emitting a continuous wave (CW) mode beam at a wavelength of 1.075 μm was used in this work. The focal position was kept to 20 mm above the work-piece to obtain a 2.2 mm spot size. The processing gases used were N₂ and ambient air (no gas) supplied at a flow rate of 25 litres/min. Programming of the laser was conducted using an SPI software which integrated with the laser system. A 50 mm line was programmed using numerical control (NC) programming as a potential beam path which was transferred by .dxf file. The nozzle indicated in Figure 4 was removed for all experiments. To obtain an operating window, trials were conducted at the fixed spot size of 2.2 mm 65 W and at a traverse speed between 10 mm/sec so that an equal comparative study of the effects of the Nd:YAG laser and the fibre laser could be performed.

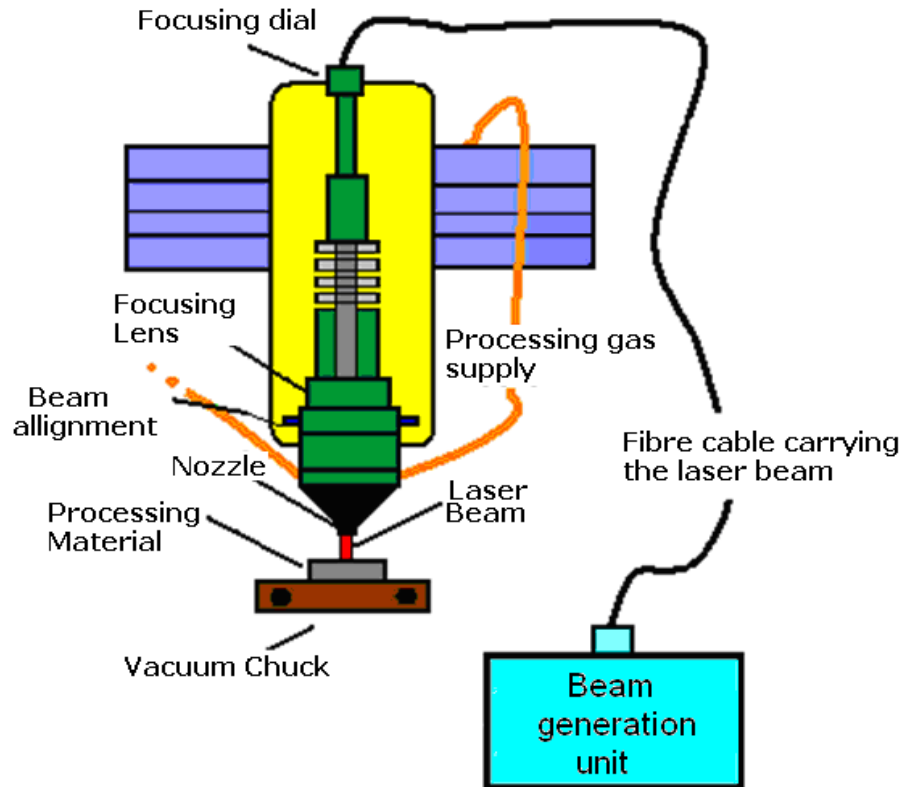


Figure 4 Schematic diagram showing the experimental set-up of the fibre laser surface treatment of the ZrO₂ engineering ceramic.

3.4 Hardness measurement

An indenter of a specific shape made from a diamond material was used to indent the Nd:YAG and the fibre laser radiated surfaces of the ZrO₂ engineering ceramics by using the Vickers (HVTM); Armstrong Engineering, Ltd. Around 50 indentation tests each were performed on all surfaces examined. An indentation load of 49.05 N was used. The indented surfaces were measured using the optical microscopy. A standardized technique was adopted to ensure that valid indentation tests were performed [25-26]. Thereafter, the surface area of the indentation (diamond foot-print) was placed into Equation 5 to calculate the hardness value:

$$HV = 2P \sin [\theta/2] / D^2 = 1.8544P/D^2 \quad (5)$$

where, P is the applied load, D is the average length of the diagonal of indentation and θ is the angle between the opposite faces of the diamond indenter.

3.5 Sample Preparation and Etching

The as-received and the laser radiated samples were mounted in epoxy resin (Epofix; Struers Ltd.) and were finely polished using a semi-automatic polishing machine (TegraPol-25; Struers Ltd.) aided by using a successively finer diamond polishing discs. The final polishing procedure was conducted by using a 0.04 μm colloidal silica suspension (OP-S; Struers Ltd.). The samples were then removed from the epoxy resin. Furthermore, the samples were etched using a thermal etching technique in order to expose the grains, to determine the grain size and investigate the microstructure. Temperature of 1300 °C was applied in a furnace to samples of the as-received, fibre and Nd:YAG laser radiated ZrO₂ engineering ceramic. The samples were held at 1300 °C for 5 min with a heating/cooling rate of 10 °C /min.

3.6 Optical Imaging

The Vickers indentation footprint of the as-received, fibre and the Nd:YAG laser radiated zones were all observed by employing the optical microscopy (Optishot; Nikon Ltd.). Further analysis was conducted by employing the field emission gun scanning electron microscopy, FEGSEM, (Ultra-high-resolution, 1530VP; Leo Ltd.) which investigated the microstructure of the laser untreated surface, Nd:YAG and fibre laser radiated surfaces of the ZrO₂ engineering ceramic.

4. Results and Discussion

4.1 Change in the Hardness

The average hardness was measured for the as-received, fibre and Nd:YAG laser radiated surfaces of the ZrO₂ engineering ceramic. The average indentation size, hardness readings along with its standard deviation (STDEV) and the ranges in the values are presented in Table 2. The average indentation size for the as-received surface was 61 µm with an average hardness of 1225 HV (12.01 GPa). This in comparison to the Nd:YAG laser radiated surface was somewhat smaller, which indicated that the Nd:YAG laser radiated surface had become more ductile and softer. The average diamond indentation size of the Nd:YAG laser radiated surface was 79 µm with an average hardness of 747 HV (7.32 GPa). A 36 % reduction in the hardness and up to 29.5 % increase in the diamond indentation size was obtained by the Nd:YAG laser radiated surface.

However, when comparing the results of the Nd:YAG laser radiated surface with that of the fibre laser radiated surface, it was found that the change in hardness was also sufficiently large but the fibre laser comprised of much higher hardness in comparison to the Nd:YAG laser radiated surface. Sufficiently large surface cracking with the fibre laser radiated sample was also found which indicated that the surface was much harder from the result of reaching high temperature which would have caused a steeper thermal gradient and rapid cooling effect to take place in comparison to the Nd:YAG laser radiation. The average size of the diamond indentation was found to be 63 µm. This in comparison to the as-received surface was just over 3 % larger but 22 % smaller in comparison to that of the Nd:YAG laser radiated surface. The average hardness of the fibre laser radiated surface was 1179 HV (11.56 GPa) which was just under 4 % lower than that of the as-received surface and 32 % higher than the Nd:YAG laser radiated surface. Figure 5 to 7 illustrates an example of the diamond indentation for the as-received surface (Figure 5), the Nd:YAG laser radiated surface (Figure 6) and the fibre laser radiated surface in Figure 7.

Table 2 Hardness values showing average, range and the STDEV found for the as-received, fibre and Nd:YAG laser radiated surfaces of the ZrO₂ engineering ceramic.

Type of Laser	Average indentation size (μm)	Range (μm)	STDEV (μm)	Hardness					
				Average		Range		STDEV	
				HV	GPa	HV	GPa	HV	GPa
As-received surface	61	57 - 68	0.00312	1225	12.01	1002 - 1414	9.83 - 13.87	12.01	1.13
Nd:YAG laser radiated surface	79	71 - 88	0.0055	747	7.32	599 - 920	5.87 - 9.02	104	1.02
Fibre laser radiated surface	63	59 - 71	0.0043	1179	11.56	920 - 1332	9.01 - 13.06	149	1.45

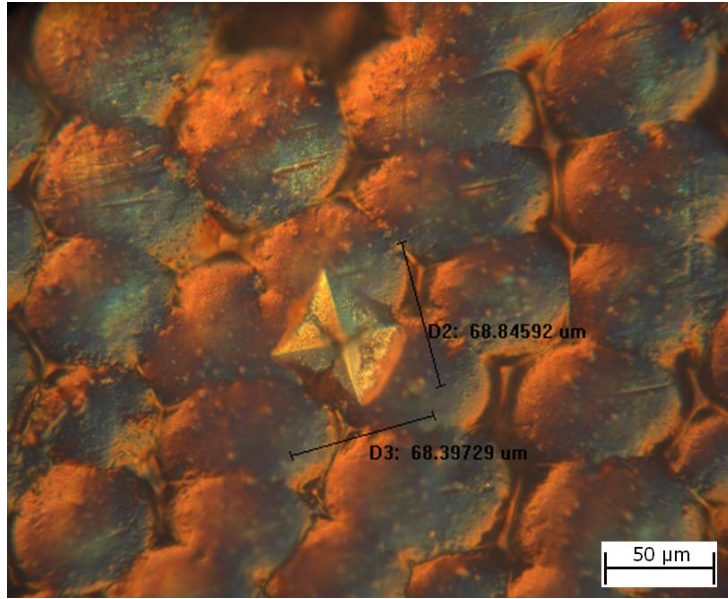


Figure 5 Optical image of the diamond indentation produced on the as-received surface indented by a 2.5 kg (24.51 N) diamond indentation load on the ZrO_2 engineering ceramic.

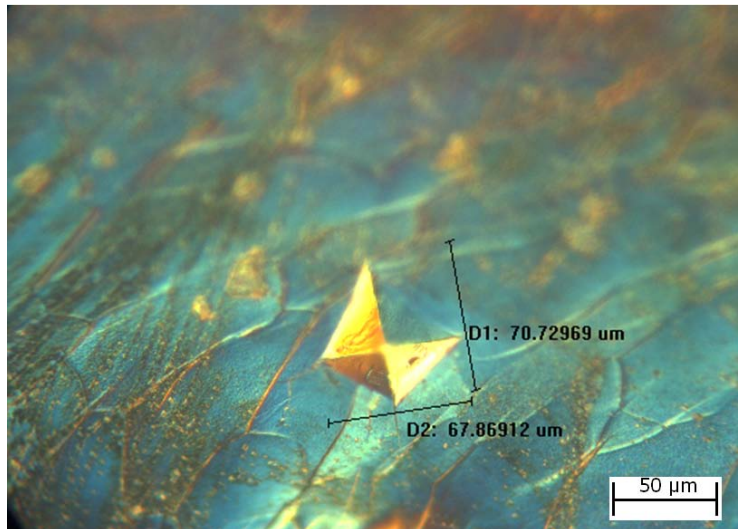


Figure 6 Optical images of the diamond indentation produced on the Nd:YAG laser radiated surface indented by a 2.5 kg (24.51 N) diamond indentation load on the ZrO_2 engineering ceramic.

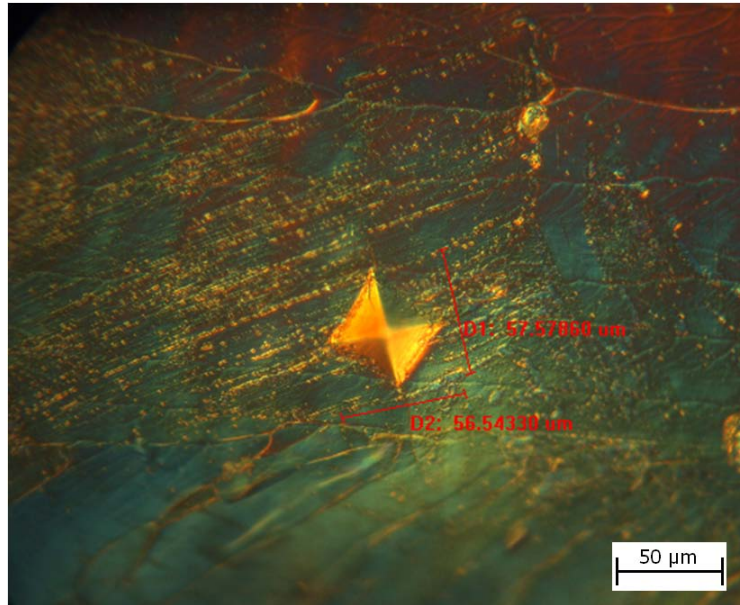


Figure 7 Optical images of the diamond indentation produced on the fibre laser radiated surface indented by a 2.5 kg (24.51 N) diamond indentation load on the ZrO₂ engineering ceramic.

4.2 Change in Size

From the topographical observation of both the Nd:YAG and fibre laser radiated track (footprint), it was found that 32 % difference in width was to be seen between the footprint created by the two lasers. The average width of the Nd:YAG laser radiated track was 632 μm with the average length of the HAZ being 72 μm. This in comparison to the track width of the fibre laser was much smaller as presented in the example in Figure 8 (a) and (b). The average width of the fibre laser radiated surface was 837 μm. The average width of the HAZ was found to be 89 μm which was 24 % higher than that of the Nd:YAG laser radiated surface.

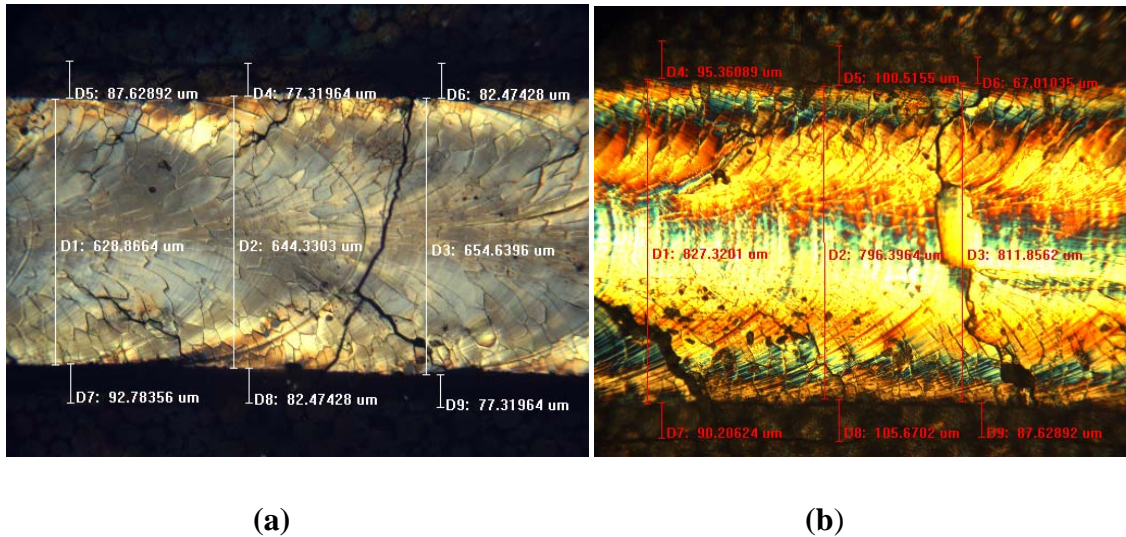
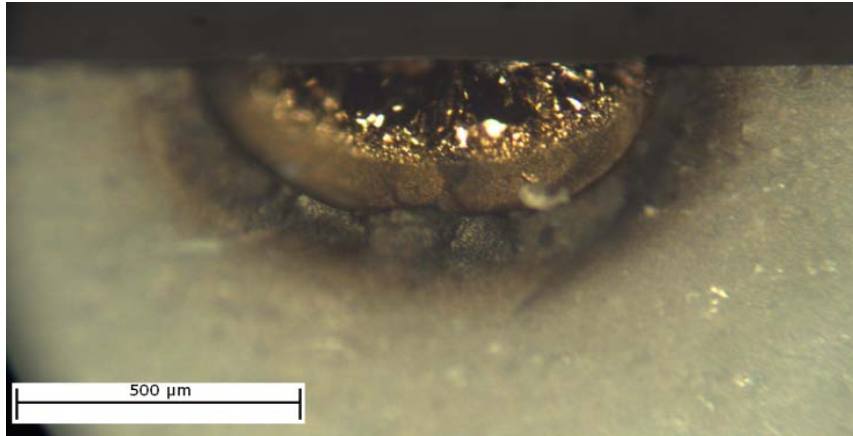
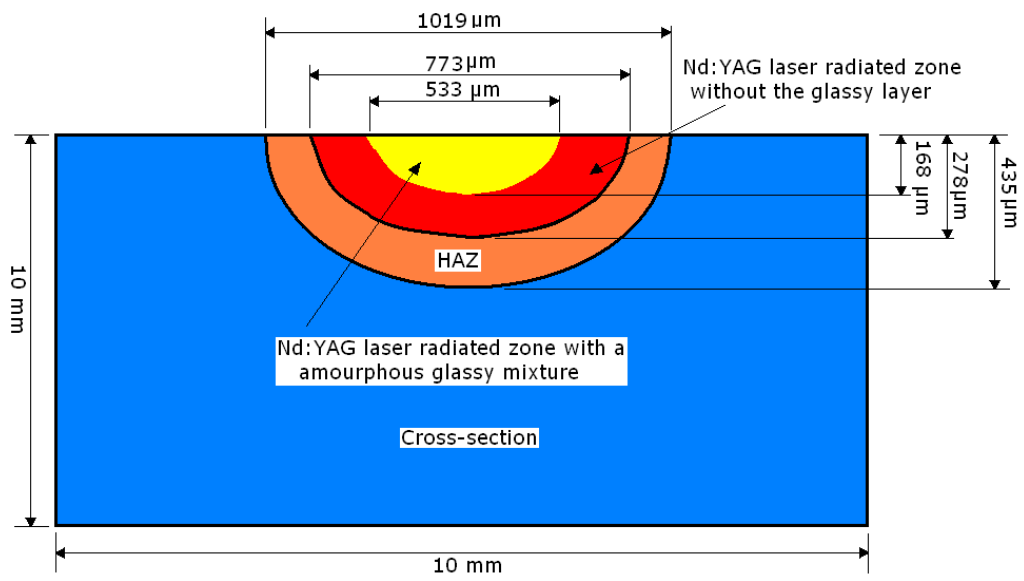


Figure 8 Optical images of (a) the width of the Nd:YAG laser radiated track and (b) the width of the fibre laser radiated track of the ZrO₂ engineering ceramic.

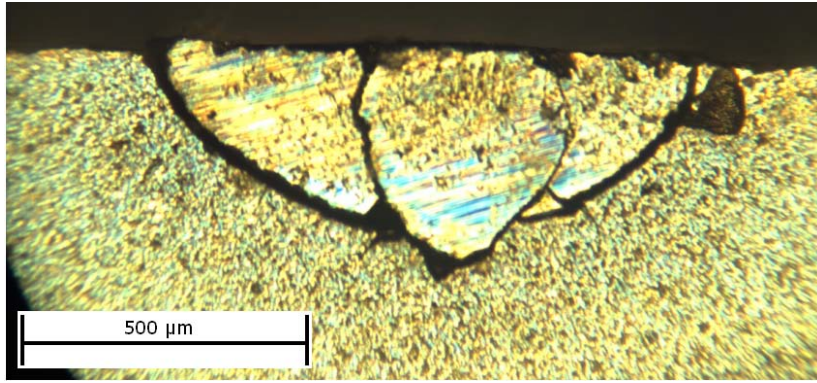
Furthermore, the optical images in Figure 9 presents of the cross-sectional view in (a) the Nd:YAG laser radiated surface and (b) the schematic of the Nd:YAG laser radiated surface with its dimensional sizes (c) fibre laser radiated surface and (d) the dimensional size of the ZrO₂ ceramic. It can be seen from the cross-sectional analysis that that the fibre laser radiated surface has produced a larger penetration depth and broader profile in comparison to that of the Nd:YAG laser. In average, the depth of penetration for the fibre laser was 447 μm as oppose to the depth of penetration of the Nd:YAG laser being 295 μm which was up to 51.5 % lower. The Nd:YAG laser had produced a partial amorphous glassy zone which was a mixture of zirconia carbon dioxide as can be seen in the image in Figure 9(a). This meant that melting did occur with the Nd:YAG laser radiated surface however, it was not as remarkable as the fibre laser radiated surface of the ZrO₂ as the whole cross-section was found to be of the amorphous glass layer. This intrinsically indicated that more melting and new formation of the surface layer had occurred with the fibre laser surface treatment despite using the same laser parameters. The increased melting and the glassy layer within the fibre laser radiated surface had occurred from the difference in temperature between the two laser as the fibre laser with a higher brightness had created much higher temperature which characteristically had melted the surface and generated a larger melt pool. The surface and the cross-sectional cracking of the ZrO₂ ceramic particularly after the fibre laser surface treatment compliments the high temperature gradients generated at the fibre laser-ZrO₂-interaction.



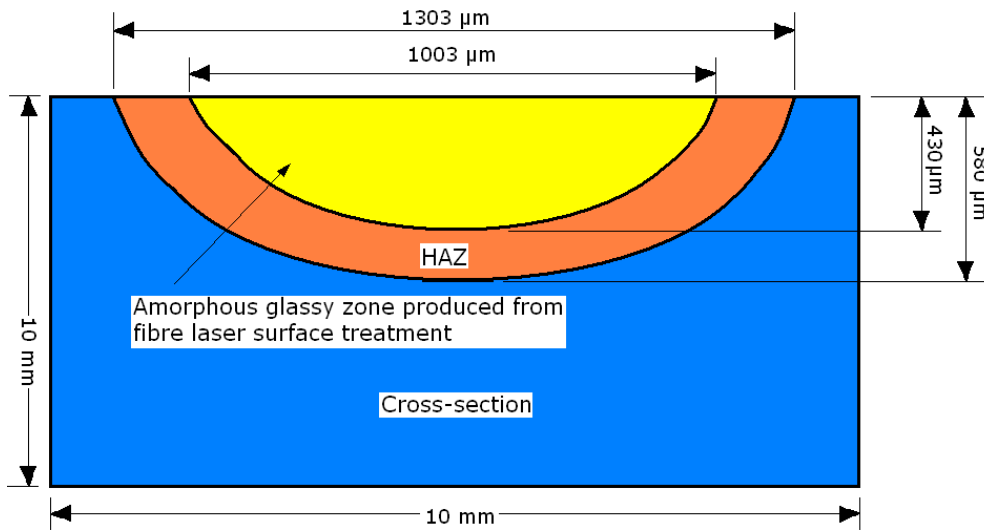
(a)



(b)



(c)



(d)

Figure 9 Optical images of the cross-sectional view of (a) the Nd:YAG laser radiated surface (b) the schematic diagram of the Nd:YAG laser radiated surface (c) the fibre laser radiated surfaces and (d) the schematic diagram of the fibre laser radiated surfaces of the ZrO_2 engineering ceramic.

4.3 Microstructural Change within the ZrO₂ engineering ceramic

4.3.1 As-received surface

The micro-structural evaluation by using the FEGSEM of the ground and polished surface of the untreated sample in Figure 10 presents the surface morphology, showing the grain boundaries along with the grain sizes. The grain size ranged between 0.7 to 0.9 μm and showed some porosity was also evident.

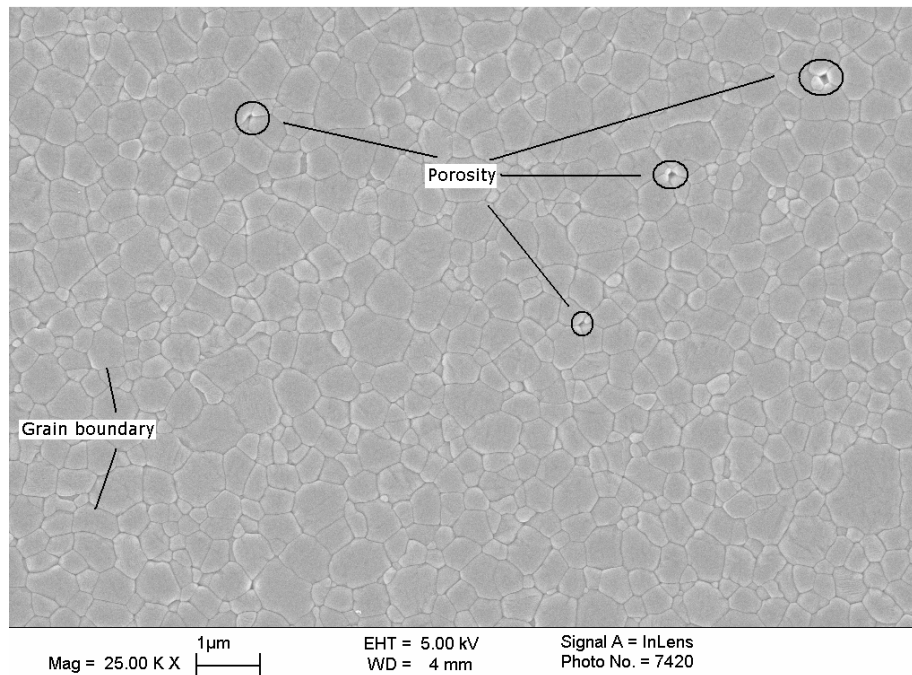


Figure 10 FEGSEM image of the as-received surface of the ZrO₂ engineering ceramic.

4.3.2. Fibre laser radiated surface

From observing the fibre laser radiated surface in Figure 11; it can be observed that the grain boundaries have enlarged and elongated on comparison to the ground and polished untreated surface. However, there is also an increase in the porosity and surface flaws in some of the regions of the fibre laser radiated surface which would have resulted from the escaping of entrapped porosity during the event of the laser interaction with the surface of the ZrO₂. Moreover, the sizes of the grains vary from 3 to 10 μm from the top (near) surface layer and through the sub-surface and the bulk of the ceramic. This is because the processing temperature at the top (near) surface layer was much higher than the sub-surface and the bulk which would have produced growth of the grains. Figure 12 presents the cross-sectional microstructure showing the increase in the grain size from the bulk of the ZrO₂ to the sub-surface and the top surface layer of the fibre laser radiated zone. The microstructure at the top

surface layer (see Figure 13 and Figure 14) is somewhat different as significant grain growth has occurred due to the high temperature gradient existing at the laser-ZrO₂-interface.

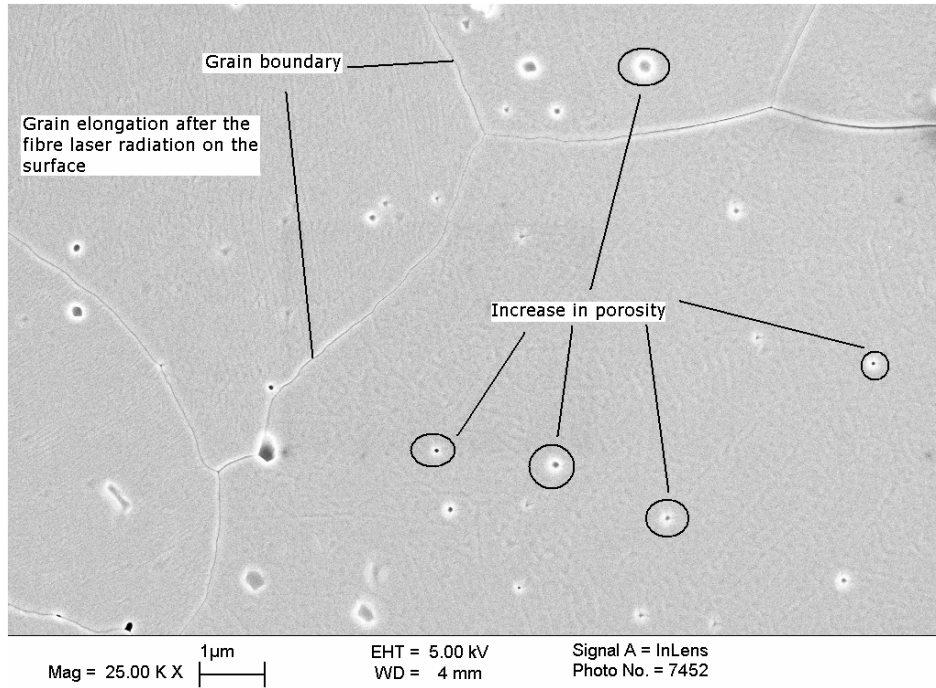


Figure 11 FEGSEM image of the cross-section sub-surface layer of the fibre laser surface treated ZrO₂ engineering ceramic.

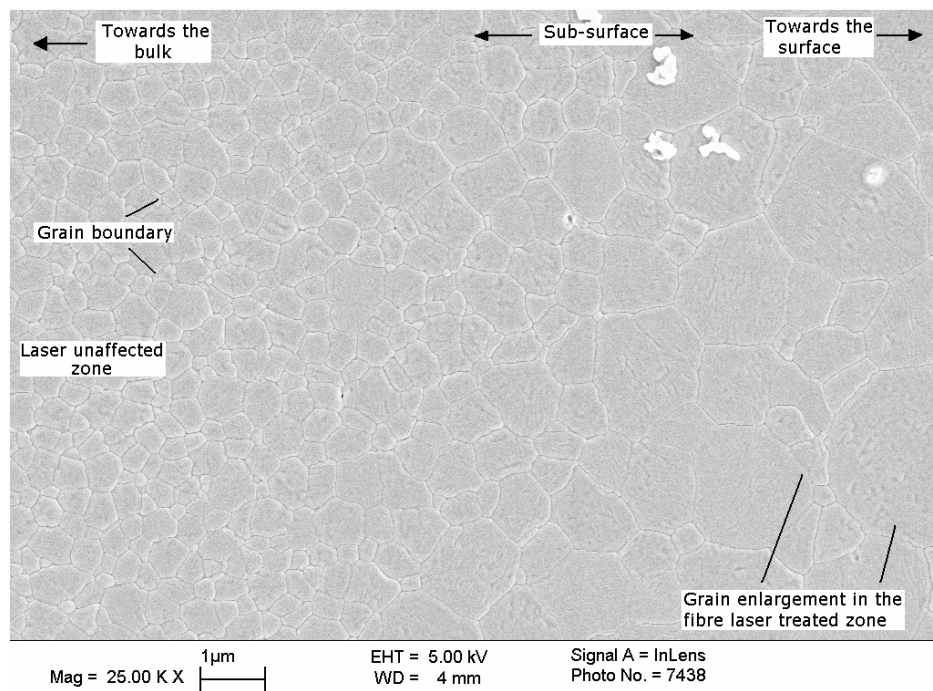


Figure 12 FEGSEM image of the cross-section of the fibre laser radiated surface of the ZrO_2 engineering ceramic showing variation in the grain sizes within the sub-surface, towards the bulk and the top surface layer.

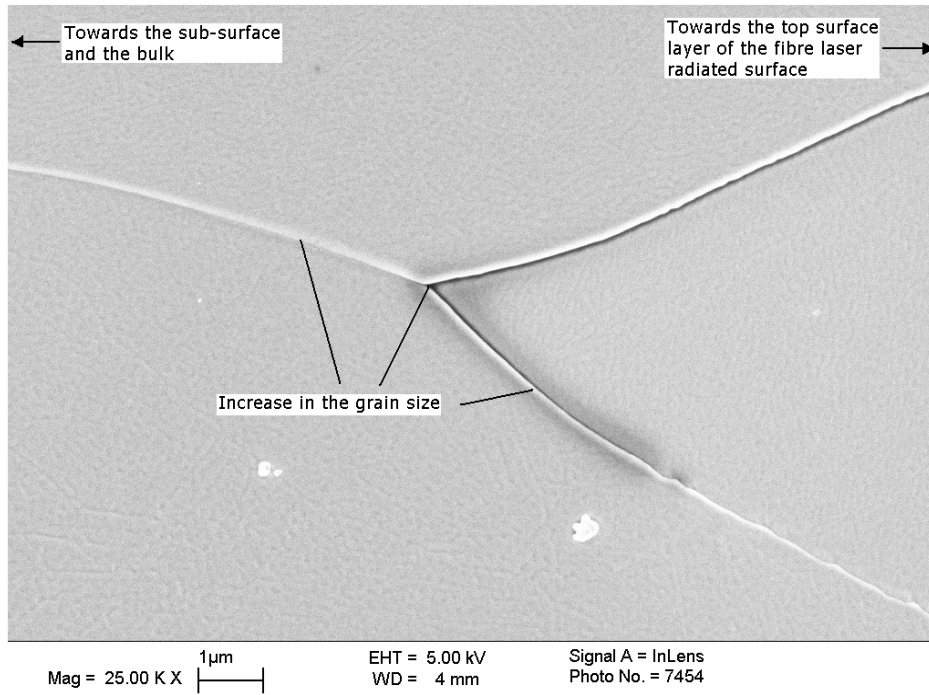


Figure 13 FEGSEM image of the cross-section of the top layer of the fibre laser radiated surface ZrO_2 engineering ceramic at x 25 K magnification.

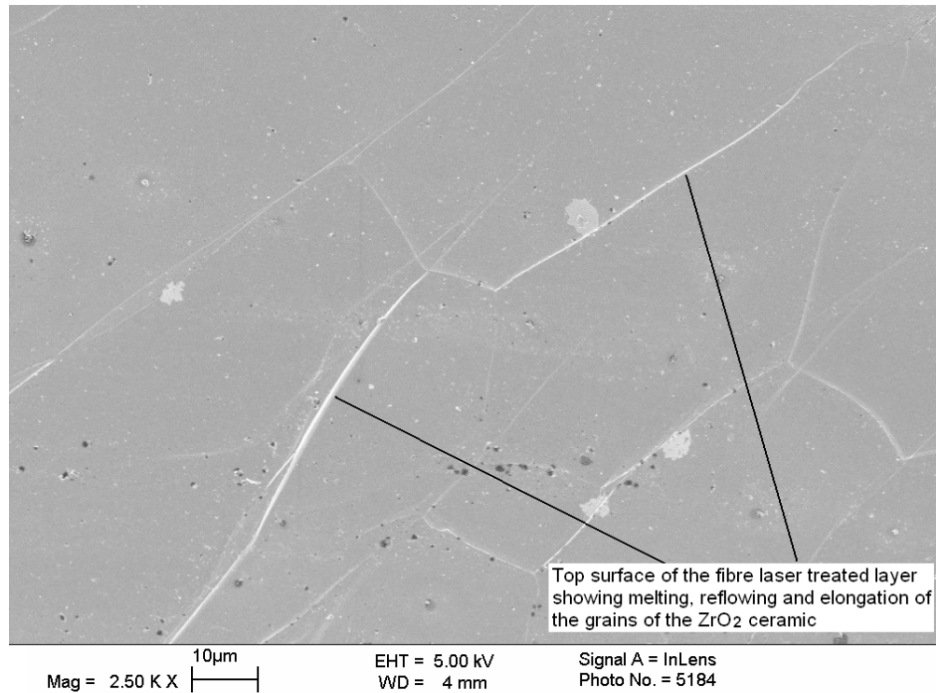


Figure 14 FEGSEM image of the cross-section of the fibre laser radiated ZrO_2 engineering ceramic illustrating the top surface layer at x 2.5 k magnification.

4.3.3 Nd:YAG laser radiated surface

The microstructure of the Nd:YAG laser radiated surface in comparison to that of the as received surface has been reasonably modified as presented in Figure 15 to Figure 17. The grain sizes herein range from about 3.5 to 7 μm with an average grain size of about 5 μm . This in comparison to the laser untreated surface was considerably large. However, when compared to the fibre laser radiated surfaces, the grain boundaries were somewhat smaller. Similar effect which occurred with the ZrO_2 samples radiated by the fibre laser also occurred with the Nd:YAG laser, although, it was slightly less significant. The sample observed at the cross-section comprised of larger grains at the top near surface layer which further reduced as it was observed at the sub-surface and the bulk of the ZrO_2 engineering ceramic as presented in Figure 15, however, this type of grain growth was slightly abnormal as elongation of the grain growth was seen in few areas. Figure 16 showed the very top surface layer of the ZrO_2 which was radiated by the Nd:YAG laser. The microstructure in this area was reasonably modified in comparison to the microstructure in where the laser interaction- ZrO_2 did not occur. Evidence of surface melting which then re-flowed and solidified can be seen particularly in Figure 16 where the laser- ZrO_2 interaction had taken place.

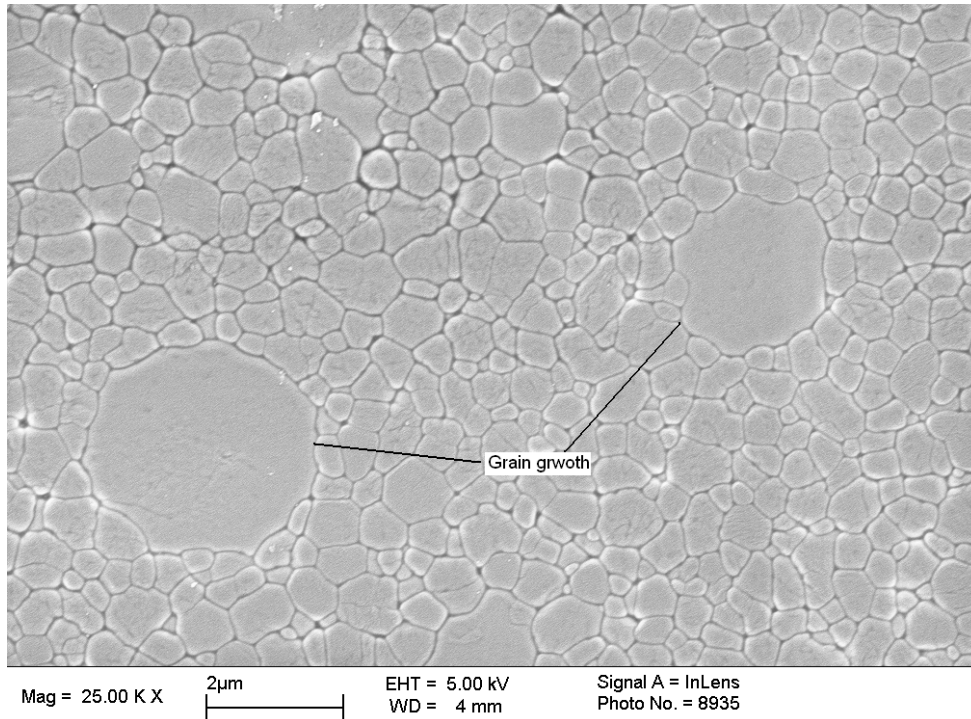


Figure 15 FEGSEM image of the cross-section of the Nd:YAG laser radiated sample of the ZrO₂ engineering ceramic within the sub-surface region.

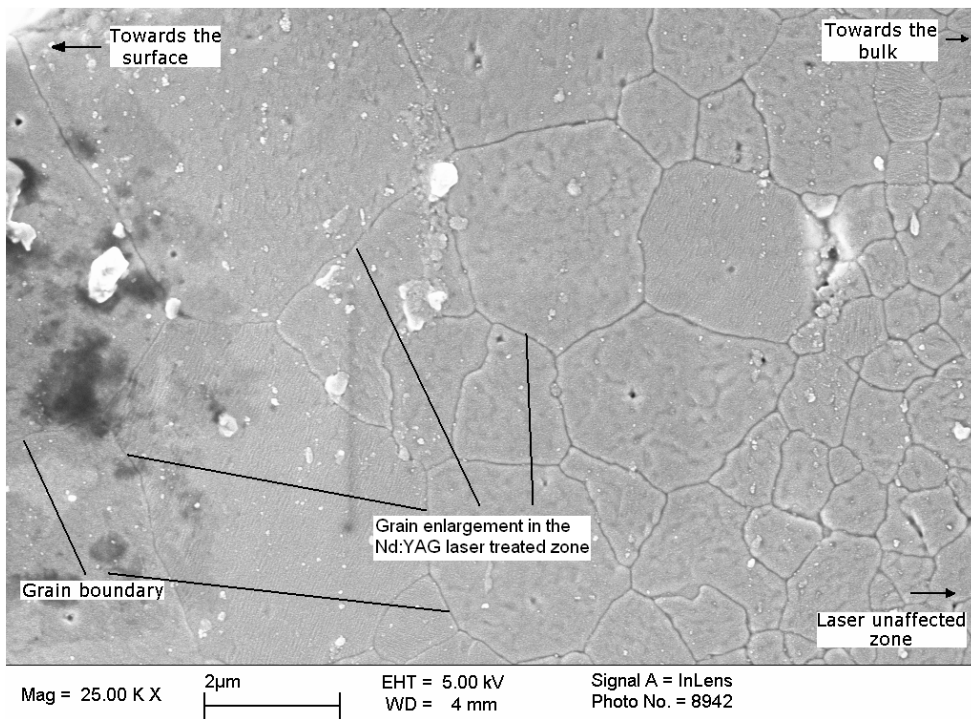


Figure 16 FEGSEM image of the cross-section of the Nd:YAG laser radiated surface of the ZrO₂ engineering ceramic illustrating the surface and the sub-surface layer.

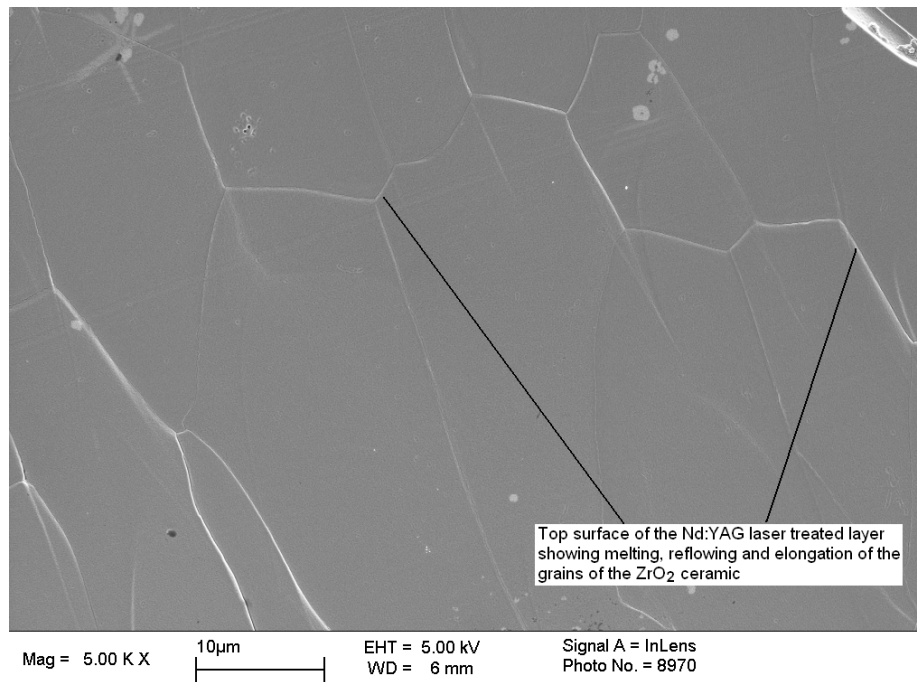


Figure 17 FEGSEM image of the cross-section of the Nd:YAG laser radiated surface of the ZrO₂ engineering ceramic illustrating the top surface layer.

4.4 Rationale and the differences between the effects produced by the two laser sources.

From the difference in the hardness values found by the results of the two laser types it can be summarized that the Nd:YAG laser radiation was producing a much softer and ductile surface to that of the fibre laser radiation. From comparing the effects of the fibre laser surface treatment and that of the Nd:YAG laser surface treatment, it is postulated that the high brightness of the fibre laser in comparison to the Nd:YAG laser would generate high temperature at the surface of the laser-ZrO₂-interface which was also supported by previous workers [16, 19]. The higher temperature has allowed the fibre laser radiated ZrO₂ ceramic to generate more melting and produced a thicker and a broader glassy layer which in turn had shown high hardness in comparison to the Nd:YAG laser radiated surface.

The change in the dimensional size was produced by the high brightness beam of the fibre laser interacting more with the ZrO₂ ceramic which in turn had generated higher processing temperatures than of the Nd:YAG laser, where as the Nd:YAG laser radiation only generated lower interaction zone as well as lower depth of penetration of the beam as seen in Figure 9(a) and (b) in comparison to Figure 9(b) and (c). This was shown by the difference in size between the footprint of the fibre and the Nd:YAG laser radiated beams (see Figure 8(a) and

(b)) and the cross-sectional images in Figure 8(a) to (d) of the Nd:YAG and the fibre laser radiated samples. As well as the depth of penetration being larger for the fibre laser in comparison to the Nd:YAG laser; the high temperature produced by the high brightness of the fibre laser had also created a larger melt zone (see section 4.2) and the amorphous glassy phase which indicated that the grain refining for both types of lasers were different as the surface of the fibre laser with larger melt-pool was producing bigger grain sizes than that of the Nd:YAG laser. This in turn generated a harder surface of the fibre laser radiated sample which was fully melted to the amorphous glassy phase as to the Nd:YAG laser which was a mixture of the amorphous glass and the zirconia oxide + carbon dioxide which on the other hand had created a softer surface as the hardness was significantly reduced.

4.5 Contribution of Laser-Beam Brightness as a Parameter to Effect Laser Surface Treatment

The brightness of a laser beam is dependent on the output power, the solid angle of divergence and the M^2 factor which are all parameters of the brightness equation as shown in section 2 in this investigation. However, laser brightness is primarily dependant on the transverse mode as well as the beam quality factor M^2 . The better the beam quality of the laser, the higher the brightness exhibited. In this case, despite the transverse mode being the same region for both the Nd:YAG and the fibre laser, the beam quality factor was a lot better for the fibre laser as there was over 5 ½ folds of difference between the beam quality factors of the Nd:YAG laser where the $M^2 = 6.8$ and the fibre laser where $M^2 = 1.2$ which showed that the fibre laser is able to produce a brighter beam. Also, the beam divergence would play a big role in increasing the brightness value as small beam divergence produces smaller solid angle of divergence ($\Omega = \pi \theta^2$). The beam quality factor therefore, allows higher brightness to be exhibited which in result had affected the change in the hardness, dimensional size and the microstructure of the ZrO_2 engineering ceramic.

The difference in the two brightness values for the Nd:YAG and the fibre laser was over 3 folds with the fibre laser comprised of high brightness but did not produce the same difference with the physical effects which took place as result of the Nd:YAG and fibre laser surface treatment. Moreover, to suggest a consistent relationship between the difference in the brightness value and the effects which take place as a result of the laser surface treatment as a quantitative value would further require experimental work. It is also suggested that the

relationship between the brightness value for two laser sources and its relative effects are unique for each ceramic as factors such as the material property as well as the absorption of the laser wavelength is considered.

As shown, that high laser-beam brightness can exhibit longer depth of penetration and bigger footprint by using identical laser power. Furthermore, it is therefore possible to operate the high brightness laser at much lower powers which in turn exhibit a surface treatment with the same dimensional size to take effect. This in the long run would help to achieve low cost per wattage laser surface treatment which is just as effective as the surface treatment applied by using a low brightness beam at higher cost per wattage. In terms of laser processing of ceramics where high powers are required for surface modification and micro-structural changes as well as phase modification where obtaining elevated processing temperature are important to create a phase change then high brightness laser such as the fibre laser is ideal.

5. Conclusions

It was found from this work that the hardness of the ZrO₂ engineering ceramic was reduced by 36 % for the Nd:YAG laser in comparison to the as-received surface - larger diamond indentation foot-prints were found which indicated that the Nd:YAG laser radiated surface had become ductile. However, only a 4 % reduction in the surface hardness was found from employing the fibre laser for surface treatment the diamond foot-prints were reduced which indicated that the fibre laser radiated surface had also become somewhat softer, although, it was not significant as much as the results of the Nd:YAG laser. The width of the fibre laser irradiated zone was also broader in comparison to the Nd:YAG laser radiated zone by 32% as well as the depth of penetration being up to 48.5 % higher for the fibre laser surface treatment. The microstructural changes also showed that the fibre laser radiated surface was producing large grains in comparison to the Nd:YAG laser radiated surface by over 20% difference in size.

The physical and micro-structural effects by applying the two laser types differed despite using identical laser processing parameters such as spot size power density, traverse speed, gas flow rate and laser wavelength. This resulted from the high brightness generated from the fibre laser radiation in comparison to the Nd:YAG laser radiation which in turn produced higher processing temperatures causing larger thermal gradient which characteristically produced a bigger melt pool. This in turn produced a harder surface in comparison to the Nd:YAG laser and caused, the increase in the width and the depth of penetration, as well as the change in the microstructure.

It can be concluded that high brightness lasers require lower powers to penetrate at equivalent dimensions to that of the low brightness lasers. This would be more cost effective since less cost per wattage is utilized. Processing of engineering ceramics is feasible and more ideal with high brightness lasers as high power densities are required, which could inherently produce a significantly modified surfaces. Experimental investigation of the effects of brightness up on laser processing is rather limited. This work is first step demonstration of what the effective results of laser brightness has up on the engineering ceramics, therefore, further work in this field would be considerably fruitful for better understanding and possibly an effective and an efficient laser surface treatment of ceramics.

6. References

1. Robieux J. *High power laser interactions*. Lavoisier Publishing: Paris. 2000
2. Milonni P.W. and Eberly J. H. *Lasers*. John Wiley & Sons, Inc: Canada, 1998.
3. Breck Hitz C. *Understanding Laser technology (2nd Edition)*. Penn Well Publishing Company: Oklahoma (USA) 1991.
4. Paschotta R. *Encyclopedia of laser, physics and Technology*. Wiley – VCH: Berlin. 2008.
5. Wilson J. Hawkes J. F. B. *Lasers Principles and Applications*. Prentice Hall International Ltd: United Kingdom. 1987.
6. Ready J. F. *Industrial Applications of lasers*. Academic Press Inc: New York. 1978.
7. Ion J. C. *Laser processing of engineering materials*, Elsevier Butterworth Heinemann: Oxford (United Kingdom). 2005.
8. Diehl R. *High Powered Diode laser fundamentals, technology, applications*. Springer Verlag: Berlin (Germany). 2000.
9. Shepelev A. V. About transforming of radiation brightness in optical processes. *American association of physics teachers* **78**(2) (2009), 158- 159.
10. Koechner W. *Solid- State laser engineering, 5th revised and updated edition*. Springer – Verlag, Berlin (Germany). 1999.
11. Das P. *Lasers and Optical Engineering*. Springer Verlag: New York. 1991.
12. British Standards. *Laser and laser-related equipment -Test methods for laser beam parameters- Beam width, divergence angle and beam*. BS EN ISO 11146. 2000

13. British Standards. *Lasers and laser-related equipment - Test methods for laser beam widths, divergence angles and beam propagation ratios - Part 1: Stigmatic and simple astigmatic beams*. BS EN ISO 11146-1. 2005.

14. British Standards. *Lasers and laser-related equipment - Test methods for laser beam widths, divergence angles and beam propagation ratios - Part 2: General astigmatic beams*. BS EN ISO 11146-2. 2005.

15. Forbes A., Burger L. and Anatolievich L. Modelling laser brightness from cross Porro prism resonators. *Laser Beam Shaping VII, Proceedings of SPIE*. **6290**(62900) (2006), M2 – M8.

16. Wallace J. Direct-diode lasers combine to form powerful, high- brightness beam. *Laser Focus World*. **June Issue** (2009), 24 – 25.

17. Wnzel H., Bernd S. and Erbert G. High brightness diode lasers. *Computers Rendus Phsique*. **4** (2003), 649 – 661.

18. Brown R. T. and Frye R. W. High-brightness laser cutting & drilling of aerospace materials. *Proceedings of ICALEO-1996, Section C*, (1996), 78 – 85.

19. Hanxuan Li., Truchan T., Brown D., Pryor R., Pandey R., Reinhardt F., Mott J., Treusch G. and Macomber S. Reliable high-efficiency high-brightness laser diode bars at 940 nm. *Optics & Laser Technology* 36 (2004), 327 – 329.

20. Treusch H. G., Ovtchinnikov A., He X., Kanskar M., Mott J. and Yang S. High - Brightness Semiconductor Laser Sources for Materials Processing: Stacking, Beam Shaping, and Bars. *IEEE Journal of selected topics in quantum electronics*, 6 (No. 4) (2000), 601 – 614.

21. Leibreich F. and Treusch H.G. (2001), *Innovative stacking techniques increase the output power and brightness of diode laser bars for materials-processing applications*. *Micro/Nano Lithography & Fabrication*. SPIE Newsroom. Retrieved

5th May 2010 <http://spie.org/x26688.xml?ArticleID=x26688>. DOI:
10.1117/2.5200109.0004.

22. Hanna D. C. Increasing laser brightness by transverse mode selection -1, Laser Techniques Series -1. *Journal of Optics and laser Technology* (1970), 122 – 125.
23. Hanna D. C. Increasing laser brightness by transverse mode selection -2, Laser Techniques Series -1. *Journal of Optics and laser Technology* (1970), 175 – 178.
24. Del Val J., Comesaña R., Lusquiños F., Boutinguiza M., Riveiro A. and Quintero F., Pou J. 2010, Laser cladding of Co-based superalloy coatings: Comparative study between Nd:YAG laser and fibre laser. *Journal of Surface & Coatings Technology*, **204** (2010), 1957–1961.
25. McColm I. J. *Ceramic Hardness*. Platinum Press, New York. 1990
26. British Standards. Vickers Hardness Test- Part 2' - *Verification and Calibration of testing Machines, Metallic Materials* - ISO 6507, 2005.